

Short Communication

Effect of scan rate on polarization curves of a high strength Al alloy in 3.5 wt% NaCl solution

Qian Liu², Qingqing Sun^{1,2,*}, Shuai Wang² and Kanghua Chen³

¹ School of Materials, Sun Yat-sen University, Guangzhou 510006, Guangdong, China

² Department of Mechanical and Energy Engineering, Southern University of Science and Technology, Shenzhen 518055, Guangdong, China

³ State Key Laboratory of Powder Metallurgy, Central South University, Changsha 410083, Hunan, China

*E-mail: sunqq7@mail.sysu.edu.cn

Received: 21 June 2021 / Accepted: 9 August 2021 / Published: 10 October 2021

The cyclic polarization curve is usually used to characterize the corrosion property of alloys, from which many parameters including potential differences which is defined as ΔE ($E_{\text{sec,corr}} - E_{\text{corr}}$) can be determined and then to assess alloys' corrosion sensitivity. Scan rate is a key but controllable parameter for cyclic polarization scan of metals. However, the effect of scan rate on ΔE has rarely been reported. 7150 Al alloy is a typical type of high strength Al alloy which is sensitive to localized corrosion. In this work, we present the effect of scan rate on ΔE of 7150 Al alloy in 3.5 wt% NaCl solution. ΔE was found increases firstly and then decreases with the increasing of scan rate. Two contradictory factors that govern the value of ΔE were discussed and the appropriate scan rate for 7150 Al alloy cyclic polarization measurement in 3.5 wt% NaCl solution was determined.

Keywords: 7150 Al alloy; Localized corrosion; Potential difference; Scan rate

1. INTRODUCTION

Because of its high specific strength and good toughness, 7150 ultrahigh strength aluminum alloy is widely used in aerospace field [1,2]. However, the alloy is prone to localized corrosion (pitting corrosion, intergranular corrosion and exfoliation corrosion), research on corrosion resistance of 7000 series aluminum alloys has attracted much attention [3-7]. The electrochemical methods are often used to rapidly evaluate the corrosion properties of metals and alloys, of which the cyclic polarization is the most common and effective method [8-10]. Polarization curves are obtained by using cyclic potentiodynamic polarization method, according to polarization curve, the electrochemical reaction

mechanism is obtained, and its shape and variation law reflect the dynamic characteristics of electrochemical corrosion process. The passivation and corrosion rate of the sample in solution can be obtained through the polarization curve. A typical cyclic polarization curve for 7150-T77 Al alloy is depicted in Fig. 1a, from which we can obtain a lot of quantitative data including corrosion potential E_{corr} , pitting potential E_{pit} , pitting transition potential E_{ptp} , corrosion current density I_{corr} and corrosion potential $E_{\text{sec,corr}}$ of reverse scan. $E_{\text{sec,corr}}$ actually corresponds to the corrosion potential occurring in the back-sweep process, which is similar to the corrosion potential E_{corr} .

Clearly, both E_{corr} and $E_{\text{sec,corr}}$ are mix potentials which determined by both anodic and cathodic reactions, thus cannot be used as a criteria to assess corrosion kinetics. But the potential difference between the two potentials, ΔE ($E_{\text{sec,corr}} - E_{\text{corr}}$), has been utilized as a criterion for decades [11-16]. Silverman proposed that for a given condition, with the increasing of the potential difference of the cyclic polarization curve, it become more and more difficult for repassivation [11,12]. However, ΔE is empirical in nature and its physical meaning is still unclear. Recently, Sun et al. [17] reported that as the corrosion current density I_{corr} changes, ΔE has a non-monotonic trend. as depicted in Fig. 1b. The corrosion current density corresponds to the corrosion fraction (F_{corr}). As the current density I_{corr} increases, the potential difference ΔE decreases firstly and then increases. For 7150 Al alloy, the relationship between ΔE and F_{corr} after cyclic polarization was obtained, as shown in Fig. 1b. According to the Fig. 1b, the corrosion can be divided into two stages, at the first stage where F_{corr} is less than one certain value ($\sim 50\%$), ΔE decreases with corrosion propagation. Then at the second stage (F_{corr} is more than the critical value), by contrast, ΔE value increases with the corrosion fraction F_{corr} which is defined as further corrosion propagation. This non-monotonic trend is true for AA 7150 under various electrolytes and temperatures.

Corrosion current is an important parameter to evaluate the corrosion rate, but it cannot be measured directly. It requires the polarization of the electrochemical system away from the equilibrium associated with the corrosion potential. Although cyclic potentiodynamic polarization method (cyclic polarization) is a common method to measure the corrosion current, there is no consensus on the selection of scanning parameters. Scan rate is a key but controllable parameter for polarization scan, this parameter is defined as the rate at which the potential of the working electrode changes relative to the reference electrode [18]. Generally the scan rate should be slow enough not only to make sure that double-layer capacitance remains fully charged but also the current collected reflects only the interfacial corrosion process at every measured potential [19,20]. Otherwise, the current obtained, not only reflects the value of current at the corrosion process but also includes the charge of surface capacitor. For instance, 0.167 mV/s is recommended in ASTM G61. However, if scan rate is too slow, the system may alter during the measurement. To sum up, in the process of electrochemical testing, it is crucial to select an appropriate scanning parameter, which may affect the credibility of experimental data. Many studies on scanning rate of electrochemical polarization curves have been reported. Shi et al. [21] studied the effects of aluminum content and potential scanning rate on pitting corrosion of AlxCoCrFeNi high entropy alloy in 3.5 wt.% NaCl solution, they proposed that the change of pitting behavior at different potential scanning rates indicated that pitting was influenced by the nature of the passivation film and the interaction between chloride ions and the active sites of the film. Fischer et al. [18] proposed a one-dimensional mathematical model of oxygen-reduced copper in a chlorine-containing medium and the

effects of scanning rate, starting overpotential and scanning direction on the characteristics of the polarization curve are analyzed. They proposed that the scan rate had an effect on the accuracy of corrosion current measurement. The results show that the error of corrosion current measurement is up to 50% under the condition of the slowest scanning rate and the maximum starting overpotential. Zhang et al. [22] studied the potential dynamic polarization curves of Ti6Al4V in naturally aerated 3.5% NaCl solution with different scanning rates. The results show that the potential is unequal to the open circuit potential when the external current density is zero. The distortion degree of polarization curve can reflect the difference between two potentials. Because of this distortion, both the values of the corrosion current density and the slope of Tafel have a large error. In addition, serious distortion of the polarization curve can lead to misunderstanding of the electrode process and a wrong conclusion. They used a new method to eliminate the distortion and analyzed the effect of charging current density on the potential. Otieno-Alego et al. [23] investigated the anodic polarization behavior at different scan rates. The effect of potential scan rate on the input parameters needed to generate anodic polarization curve was established by model calculation, and an empirical linear relationship was derived. It has been found from previous reports that there have been many studies on the effect of scanning rate on polarization curve. However, there are few studies between quantitative data points of polarization curve and the scanning rate, there are almost no reports on the relationship between the potential difference and scanning rate in the polarization curve.

In our work, the cyclic polarization tests of 7150 Al alloy under naturally aerated 3.5 wt% NaCl solution were conducted, and at different scan rates (from 100 to 0.1 mV/s). Different scan rates lead to different degree of damage on alloy's surface during anodic polarization, and the relationship between ΔE ($E_{\text{sec,corr}} - E_{\text{corr}}$) and corrosion fraction (F_{corr}) will be investigated and discussed.

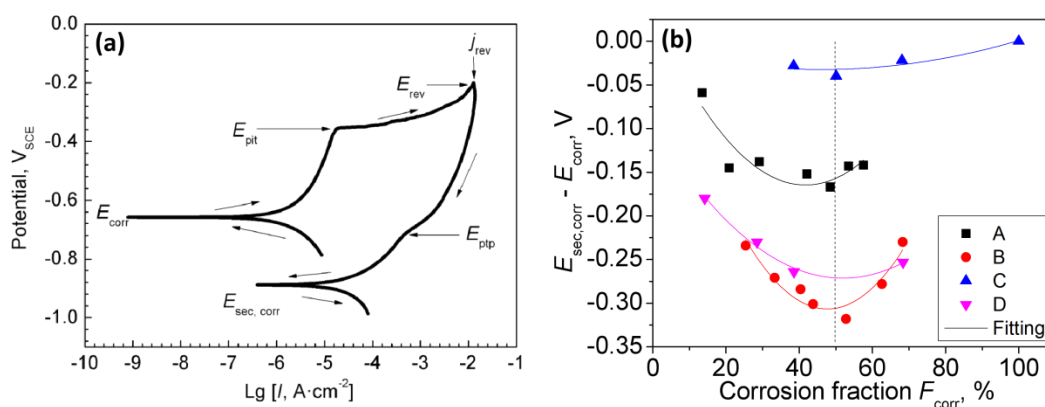


Figure 1. (a) Schematic representation of the quantitative parameters of cyclic polarization curve [17]. The cyclic polarization curve corresponds to polished 7150-T77 Al alloy in naturally aerated 0.1 mol/L Na₂SO₄ + 20 mmol/L NaCl solution with $E_{\text{rev}} = -0.2$ V_{SCE}. (b) The relationship between ΔE ($E_{\text{sec,corr}} - E_{\text{corr}}$) and corrosion fraction, ΔE as a function of surface corrosion fraction F_{corr} after cyclic polarization test for group A, B, C and D, respectively [17]. When the corrosion fraction equals approximately 50%, a turning point can be seen.

2. EXPERIMENT

2.1. Materials preparation

The investigated material was a cold-rolled 7150 Al alloy plate and treated with T77 ageing process. The chemical composition, optical microstructure and surface finishing can be found in elsewhere [24].

2.2. Cyclic polarization and corrosion morphology

Cyclic polarization measurements were performed on a CHI 660C electrochemical workstation (Shanghai Chenhua, China) using a three-electrode cell. The working electrode was AA 7150 that fixed in a holder with an exposing area of 0.5 cm², platinum plate was used as the counter electrode, and saturated calomel electrode (SCE) for the reference electrode. After 1 h pre-immersion, cyclic polarization tests were carried out in naturally aerated 3.5 wt% NaCl solution in a Faraday cage, with the scan rates changed from 100 to 0.1 mV/s. The corrosion morphologies of the alloy after the electrochemical test were observed by optical microscopy (LEICA NEOPHOT-21). What's more, scan rate is a factor that can influence the surface corrosion degree. The corrosion degree of the surface region is promoted by slower scan rate. We can use corrosion fraction (F_{corr}) to define the corrosion degree, F_{corr} is the ratio of the dark area to the whole area of a sample. The method of calculating surface corrosion fraction of a sample after electrochemical test was described elsewhere [17].

3. RESULTS AND DISCUSSION

The shapes of polarization curves at different scan rates are different. Fig. 2 shows the cyclic polarization curves of 7150 Al alloy in naturally aerated 3.5 wt% NaCl solution. Values of E_{pit} and E_{ptp} with different scan rate are listed in Table 1. At higher scan rates, E_{pit} and E_{ptp} are absent in cyclic polarization curves, i.e., E_{pit} is not shown up for 50 and 100 mV/s; E_{ptp} is not shown for scan rate higher than 1 mV/s. It is also can be seen is that E_{pit} gradually shifts to the negative direction with slower scan rate. And for the two slowest scan rate 1 and 0.1 mV/s, E_{pit} stabilizes at the same value (-0.715 V_{SCE}). However, E_{ptp} changed dramatically at 1 and 0.1 mV/s.

After electrochemical polarization test, the value of corrosion fraction was calculated by a ImageJ2x software. To ensure the repeatability of the experiment and the reliability of the data, here we calculated the corrosion fraction (F_{corr}) by using at least 5 images for each experimental point. From the corrosion morphologies shown in Fig. 3, it can be seen that the corrosion fraction of 7150 Al alloy at the scan rate of 1 mV/s and 0.1 mV/s is 33% and 46%, respectively (corresponding to the first corrosion stage where F_{corr} is less than one certain value (~50%) in Fig. 1b).

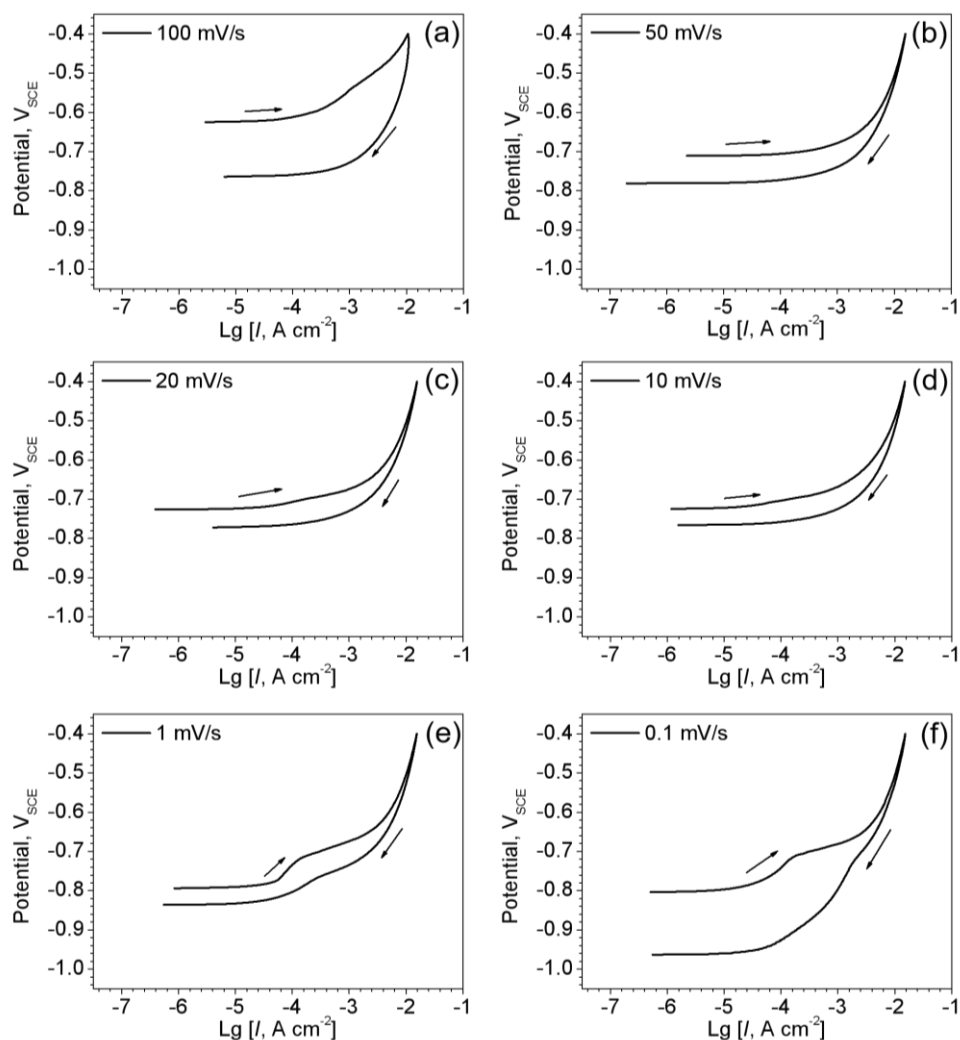


Figure 2. Anodic cyclic polarization curves of 7150 Al alloy in naturally aerated 3.5 wt% NaCl solution with the change of scan rates: (a) 100 mV/s, (b) 50 mV/s, (c) 20 mV/s, (d) 10 mV/s, (e) 1 mV/s, (f) 0.1 mV/s. (Note that cyclic polarization curves at scan rates higher than 10 mV/s were obtained using CV (Cyclic Voltammetry) firstly, and then transformed CV curves into cyclic polarization curves by plotting the potential as a function of $\log I$.)

Table 1. Values of E_{pit} and E_{ptp} with the change of scan rate

Scan rate, mV/s	100	50	20	10	1	0.1
$E_{\text{pit}}, \text{V}_{\text{SCE}}$	/	/	-0.697	-0.708	-0.715	-0.715
$E_{\text{ptp}}, \text{V}_{\text{SCE}}$	/	/	/	/	-0.767	-0.722

So merely based on the relationship between ΔE ($E_{\text{sec,corr}} - E_{\text{corr}}$) and corrosion fraction: the potential difference decreases at first and then increases with an increase of corrosion fraction[17], it can be expected that, for the studied scan rate range, the value of ΔE would increase monotonically with higher scan rate.

However, the experimental results are inconsistent with the expectation. As depicted in Fig. 4, the value of ΔE only shows the expected upward trend at the scan rate ranging from 0.1 to 1 mV/s; whereas the results ranging from 1 to 100 mV/s does not meet the expectation. The reason is that a very high scan rate would cause non-faradaic current and leave less time for data collecting system. At least $10R_uC_d$ is needed for a full establishment of a potential step (R_uC_d is the cell time constant, $5R_uC_d$ for charging of double layer capacitance and another $5R_uC_d$ for taking data). If the scan rate is not low enough, some of the current generated would reflect charging of the surface capacitance in addition to the corrosion process. Thus, the measured current would be greater than the current actually generated by the corrosion reactions, thus could not reflect the real corrosion process. This non-faradaic effect together with the current delay in data collecting system (Data collecting lag effect) lead to the result that the potential collected shifts to the forward direction, i.e., E_{corr} and E_{pit} shift to more anodic direction and $E_{\text{sec,corr}}$ shifts to more cathodic direction. As a result, for high scan rate range, $(E_{\text{sec,corr}} - E_{\text{corr}})$ decreases with the accelerated scan rate.

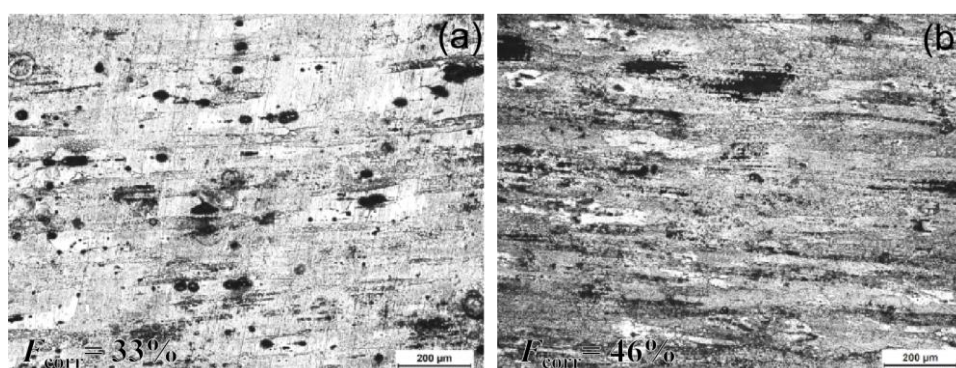


Figure 3. Corrosion morphologies of 7150 Al alloy after electrochemical tests with different scan rates in naturally aerated 3.5 wt% NaCl solution: (a) 1 mV/s; (b) 0.1 mV/s. The corrosion fraction (F_{corr}) is 33% and 46%, respectively.

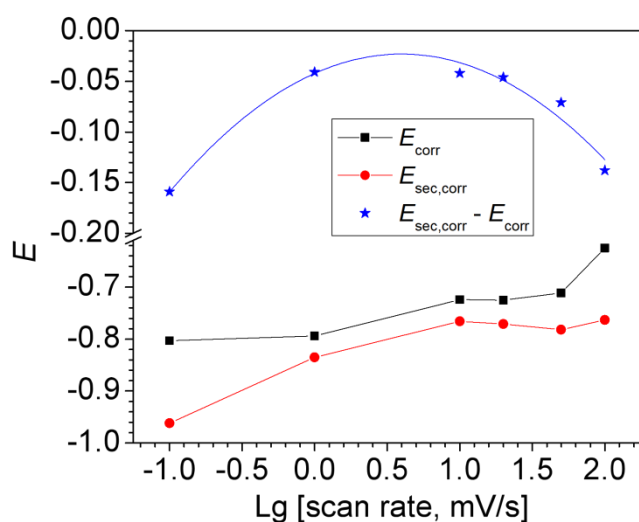


Figure 4. E_{corr} , $E_{\text{sec,corr}}$ and ΔE ($E_{\text{sec,corr}} - E_{\text{corr}}$) of 7150 Al alloy with different scan rate in naturally aerated 3.5 wt% NaCl solution.

Therefore, two contradictory effects might be caused by scan rate, as listed below:

(A) Slower scan rate results in more corroded surface, indicating the value of ΔE increases with higher scan rate (F_{corr} is less than 50% for the lowest studied scan rate).

(B) Non-faradaic and data collecting lag effect led to ΔE decreases with higher scan rate.

For lower scan rates (0.1 and 1 mV/s) at which non-faradaic effect can be neglected, the ΔE value is predominantly influenced by effect A. Thus, as expected, ΔE increases with higher scan rate. For alloys with scan rate higher than 20 mV/s (20, 50, 100 mV/s), the corroded surface area would be relatively a constant and the non-faradaic effect would play the main role in determining the value of ΔE (effect B). As a result, the ΔE becomes more negative as scan rate increases from 20 mV/s to 100 mV/s. For the intermediate scan rates (1, 10, 20 mV/s), ΔE value is stable at ~ 0.05 V, which is due to that at this range, ΔE is determined by the two contradictory effects and a balance achieved between them (effect A and B).

Generally, it is worth noting that the lower scan rate is necessary if the alloy is in passive stage or if it is corroded at a lower corrosion rate. The polarization being measured should be without interference from the capacitance. However, it is also generally accepted that the scan rate should not be so low so as to make them impractical. Moreover, on the other hand, if scan rate is too slow, the test system may change during the measurement, as proposed by Poursaei [19]. It has been proved by a large number of experiments that the scanning rate not only affects the shape of polarization curve, but also the corrosion potential and pitting potential [25,26]. Therefore, if the scan rate value selected is not correct, it will result in an incorrect interpretation. The most appropriate scan rate should be the maximum scan rate at which the charging of the surface capacitance can be ignored. Maximum scan rates for several polarization resistance values, solution resistance values and capacitance values have been calculated according to the break point data in Bode plot [27, 28]. For frequencies lower than the break point, the capacitor is already fully charged, thus the contribution is only from resistor (corrosion process only) [19, 27, 28]. If the corrosion process can be seen as a resistor (solution resistance R_{Ω}) and a combination of a resistor and capacitor (polarization resistance R_p and double-layer capacitor C_{dl}), then the frequency at the break point (f_b) can be described by Eq. (1):

$$f_b = \frac{1}{4\pi R_{\Omega} C_{dl}} \left\{ 1 - \frac{1}{R_p} \sqrt{R_p^2 - 4R_{\Omega} R_p - 4R_{\Omega}^2} \right\} \quad (1)$$

The applied frequency should be about an order of magnitude lower than the breakpoint frequency [19]. And the maximum scan rate S_{max} can be estimated by using Eq. (2):

$$S_{max} = [\pi V_{pp} f_{max}] < \left[\frac{\pi V_{pp} f_b}{10} \right] \quad (2)$$

where V_{pp} is the peak-to-peak amplitude. For the studied 7150 Al alloy in 3.5 wt% NaCl solution, f_b is about 1 Hz, V_{pp} equals to 10 mV [29]. According to Eq. (2), the estimated maximum scan rate S_{max} for the studied system is 3.1 mV/s.

Experimentally, as depicted in Fig. 2, when the scan rate changes from 1 to 0.1 mV/s, the E_{corr} and current density values stay relatively constant, indicating that the charging of the surface capacitance can be ignored at the scan rate of 1 mV/s. So that the most appropriate scan rate should be no less than 1 mV/s for the corrosion of 7150 Al alloy in 3.5 wt% NaCl. On the other hand, in 3.5 wt% NaCl solution, pitting potential of 7150 Al alloy is a critical parameter which can only be obviously seen when scan rate is 0.1 and 1 mV/s. It is reasonable to predict that there is a maximum scan rate lying between 1 and

10 mV/s at which obvious pitting potential can be observed. Therefore, in terms of surface capacitance and pitting potential, the experimental results indicate that the appropriate scan rate lies between 1 and 10 mV/s for 7150 Al alloy in 3.5 wt% NaCl solution. This is in agreement with the calculated value (3.1 mV/s).

4. CONCLUSION

In the studied scan rate range, ΔE ($E_{\text{sec,corr}} - E_{\text{corr}}$) of 7150 Al alloy in 3.5 wt% NaCl solution increases firstly and then decreases with the increasing of scan rate. Two contradictory factors govern the change of ΔE : (1) Non-monotonic relationship between ΔE and corrosion degree indicates that the value of ΔE would increase with higher scan rate; (2) Non-faradaic effect and data collecting lag effect would lead to a decrease of ΔE with higher scan rate. The appropriate scan rate for cyclic polarization measurement of 7150 Al alloy lies between 1 and 10 mV/s in the 3.5 wt% NaCl solution, according to experimental and calculation results.

ACKNOWLEDGEMENTS

The authors are happy to acknowledge financial support from National Key Research and Development Program of China (No.2016YFB0300801). The financial support of the China Scholarship Council is also gratefully acknowledged.

References

1. A Heinz, A Haszler, C Keidel, et al, *Mater. Sci. Eng. A*, 280(1)(2000) 102.
2. H.X. Li, Q.L. Bai, Y. Li, Q. Du, L. Katgerman, J.S. Zhang, L.Z. Zhuang, *Mater. Sci. Eng. A*, 698 (2017) 230-237.
3. R. Arrabal, B. Mingo, A. Pardo, M. Mohedano, E. Matykina, I. Rodríguez, *Corros. Sci.*, 73(2013) 342-355.
4. S. Chen, K. Chen, G. Peng, L. Jia, P. Dong, *Mater. Des.*, 35(2012) 93-98.
5. Q. Sun, R. Xu, Q. Han, K. Zhao, I. McAdams, W. Xu, *Appl. Mater. Today*, 14(2019) 137-142.
6. B. Wang, Y. Su, X. Mou, Y. Xiao, J. Liu, *Mater. Des.*, 50(2013) 15-21.
7. Q. Sun, Q. Han, R. Xu, K. Zhao, J. Li, *Corros. Sci.*, 130(2018) 218-230.
8. S. S. Jamali, S. E. Moulton, D. E. Tallman, M. Forsyth, J. Weber, G. G. Wallace, *Corros. Sci.*, 86(2014) 93-100.
9. Q. Sun, X. Liu, Q. Han, J. Li, R. Xu, K. Zhao, *Surf. Coat. Technol.*, 337(2018) 552-560.
10. J. Izquierdo, S. González, R. M. Souto, *Int. J. Electrochem. Sci.*, 7(2012) 11377-11388.
11. D.C. Silverman, *Uhlig's Corrosion Handbook*, 1129(2011).
12. R. McGuire, D. Silverman, *Corros.*, 47(1991) 894.
13. B. Zaid, D. Saidi, A. Benzaid, S. Hadji, *Corros. Sci.*, 50(2008) 1841.
14. U. Trdan, J. Grum, *Corros. Sci.*, 59(2012) 324.
15. M. Finšgar, I. Milošev, *Corros. Sci.*, 52(2010) 2430.
16. M. Dabala, K. Brunelli, E. Napolitani, M. Magrini, *Surf. Coat. Technol.*, 172(2003) 227.
17. Q. Sun, K. Chen, *J. Electrochem. Sci. Technol.*, 11(2) (2020) 140-147.
18. D A Fischer, I T Vargas, G E, Pizarro et al, *Electrochim. Acta*, 313(2019) 457-467.

19. A. Poursaee, *Electrochim. Acta*, 53 (2010) 1200.
20. H. Leckie, *J. Electrochem. Soc.*, 117 (1970) 1152.
21. Y Shi, B Yang, X Xie, et al, *Corros. Sci.*, 119(2017) 33-45.
22. X.L. Zhang, Z.H. Jiang, Z.P. Yao, Y. Song, Z.D. Wu, *Corros. Sci.*, 51(2009) 581-587.
23. V. Otieno-Alego, G.A. Hope, H.J. Flitt, G.A. Cash, D.P. Schweinsberg, *Corros. Sci.*, 33(1992) 1719-1734.
24. Q. Sun, J. Hu, J. Li, K. Chen, P. Dong, X. Liao, Y. Yang, *Int. J. Electrochem. Sci.*, 12 (2017) 5363.
25. SL de Assis, S Wolyneć, I Costa, *Electrochim. Acta.*, 51(8–9) (2006) 1815-1819.
26. M. Stern, A.L. Geary, *J. Electrochem. Soc.*, 104 (1) (1957) 56–63.
27. D.C. Silverman, NACE International, Houston, TX (United States), 1998.
28. F. Mansfeld, M. Kendig, *Corrosion*, 37(1981) 545.
29. Q. Sun, K. Chen, H. Fang, J. Xu, P. Dong, G. Hu, Q. Chen, *Int. J. Electrochem. Sci.*, 11(2016) 5855.

© 2021 The Authors. Published by ESG (www.electrochemsci.org). This article is an open access article distributed under the terms and conditions of the Creative Commons Attribution license (<http://creativecommons.org/licenses/by/4.0/>).